The Dynamics of Granular Flow in Hopper Silos

Hagos Eman, Dr. Timothy Newson, and Dr. Aly Ahmed
Geotechnical Research Centre
Civil and Environmental Engineering, University of Western Ontario
London, ON, Canada

GeoVirtual 2020 September 14-16
Resilience and Innovation

ABSTRACT

Particle Image Velocimetry (PIV) based experimental tests have been used to investigate the granular flow properties in a half model smooth-sided silo hopper. This paper shows that the flow patterns and dynamic flow properties of a model silo system under natural gravity can be effectively captured using PIV. The technique appears to be a valuable additional tool for practical and experimental capture of the material flow. The results in the paper show that the flow mechanisms in a silo are quite complex and vary temporally and spatially. Three distinct zones of behaviour were observed: a) an upper inflow zone, b) a narrow vertical funnel flow zone and c) a near static stagnant zone. The characteristics of these flow zones are likely to be influenced by the material and geometric properties of the silo. Additional testing will be conducted by the researchers with other materials, silo geometries and enhanced gravities in the centrifuge, to further understand the physical processes involved and the limitations of the experimental methods.

RESUME

Des tests expérimentaux basés sur la vélocimétrie par image des particules (PIV) ont été utilisés pour étudier les propriétés d'écoulement granulaire dans une demi-trémie de silo à parois lisses. Cet article montre que les modèles d'écoulement et les propriétés d'écoulement dynamique d'un système de silo modèle sous gravité naturelle peuvent être efficacement capturés à l'aide de PIV. La technique semble être un outil supplémentaire précieux pour la capture pratique et expérimentale du flux de matière. Les résultats de l'article montrent que les mécanismes d'écoulement dans un silo sont assez complexes et varient temporellement et spatialement. Trois zones de comportement distinctes ont été observées: a) une zone d'entrée supérieure, b) une zone d'écoulement en entonnoir vertical étroit et c) une zone stagnante presque statique. Les caractéristiques de ces zones d'écoulement sont susceptibles d'être influencées par les propriétés matérielles et géométriques du silo. Des tests supplémentaires seront effectués par les chercheurs avec d'autres matériaux, des géométries de silos et des gravités améliorées dans la centrifugeuse, pour mieux comprendre les processus physiques impliqués et les limites des méthodes expérimentales.

1 INTRODUCTION

Dense fluid-particle flows in which the direct particle-particle interactions are a dominant feature encompass a diverse range of industrial and geophysical contexts including, for example, slurry pipelines (Shook and Roco, 1991); granular material storage (Nortje, 2002); fluidized beds (Davidson and Harrison, 1971); mining and milling operations, ploughing (Brennen, 2005); abrasive water jet machining, food processing, debris flows (Iverson, 1997); avalanches (Hutter *et al.*, 1993); landslides, sediment transport and earthquake-induced soil liquefaction (Hughes and Madabhushi, 2019).

Silos with conical hopper bases have been used for centuries to store and handle bulk materials in areas of food processing, mining, and chemical operations. Many research works refer to the importance of the experimental and analytical study of wall pressure distributions and flow analysis for different geometries (Nortje, 2002). In most cases, failures occur due to inadequate design analysis of the dynamic behaviour of the bulk material during the discharge of the hopper (Yong, 1990). Some common problems in hopper granular flow are arching, funnel flow with wide residence time distribution and deterioration in product quality, ratholing, segregation, vibration and noise (Schulze, 2007). Many approaches have been followed to better understand granular flow in these systems, such as analytical methods, numerical modeling (finite element method and discrete element methods), and experimental full scale and reduced scale tests.

The velocity field and mass flow rate of granular flow inside hoppers has been characterized using stress and density based critical-state soil mechanics (Prakash and Rao, 1991) by imposing velocity discontinuities across the hopper. Although this approach provided some insights, the resulting mathematical equations were ill-posed and show indeterminacy in the stress tensors, which resulted in strong singularities (Pitman and Schaeffer, 1987). A second approach that ignores the stress field and creates a purely kinematic description of the velocity field, was proposed by Litwiniszyn (1963), with an empirical constitutive law combined with a random walk method. Caram and Hong (1991) modified a stochastic void model originally devised by Mullins (1972) and implemented it explicitly in computer simulations on a triangular lattice Nedderman and Tüzün (1979) based their approach on another constitutive model involving velocity gradients and although it performs well for certain cases, Medina *et al.* (1998) and other researchers found that it does not fully capture the kinematic behaviour properly when the silo is

analyzed in detail with particle image velocimetry (Choi *et. al.*, 2005).

Measurements of flow patterns in full-scale silos is very rare and observations are typically based on changes in the top surface profile, outflow rate measurements and signs of abrasion and polishing of the walls (Ooi *et al.*, 1998). Most velocity field and flow pattern studies have therefore utilised laboratory models. These approaches are small enough to allow novel visualization techniques, such as spy-holes, transparent walls. radio transmitters, X -rays and positron emission. etc. (e.g. Bransby and Blair-Fish, 1974; Rotter *et al.*, 1989). However, the effect of stress levels on the flow behaviour are extremely important and extrapolation of these observations conducted under natural gravity to full-scale is uncertain. The friction, density and flow properties of a granular material are related to the self-weight, normal contact forces and tangential forces, and stresses experienced in models are generally much smaller than those experienced in full-scale silos. Some of these challenges can be addressed by using an enhanced gravity field for the model (e.g. placing it into a large centrifuge) and the criteria for modelling similarity has been defined by Nielsen and Askegaard (1977). A limited number of studies have been conducted using centrifuge-based silos (Mathews and Wu, 2016; Nielsen and Askegaard, 1977; Barbir and Mathews, 2016). Material discharge from silos may be better understood by investigating these internal flow patterns and the effects of gravity (both natural and enhanced). However, this has not yet been widely investigated and this is undoubtedly due to the challenges associated with making quantitative observations of the internal flow. Hence, uncertainties still exist about the complex velocity fields that occur within silos during material discharge, which makes many of the former analytical and numerical predictions somewhat speculative and design of these structures difficult.

1.1 Silos and Silo Granular Flow

Silos can be characterized based on their qualitative flow patterns. Jenike (1961) defined the basic flow patterns as mass and funnel flow as shown in Figure 1. Mass flow occurs when the whole particulate material moves simultaneously during discharge. In funnel flow, the material in the central region of the hopper exits first, followed by the material closest to the walls of the hopper.

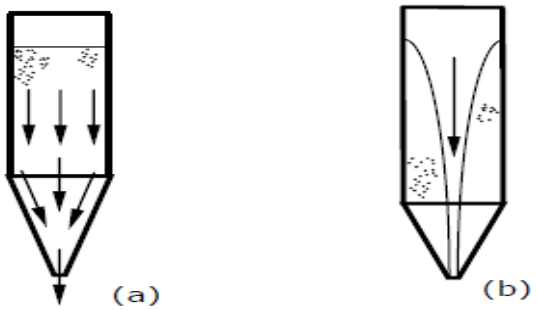

Figure 1: (a) mass flow (b) funnel flow

The resulting flow type is a complex interaction between material properties and the geometry of the silo. A Jenike Diagram taken from Schulze (2007) is shown in Figure-2 and shows how the behaviour transitions from one form of flow to the other, dependent on the conical hopper angle

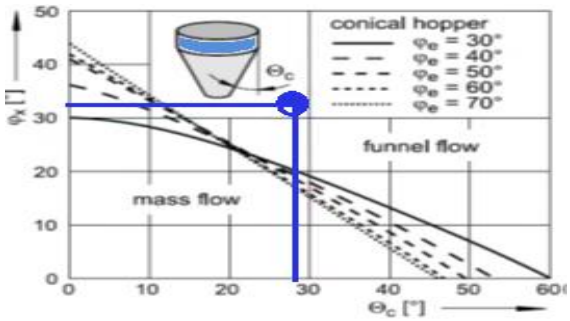

Figure 2: Flow pattern from (Schulze, 2007)

(θ_c), wall friction angle (φ_e) and the material friction angle (φ_x). The blue color line shown in the figure, provides an example of a material with friction angle of 32^o and hopper angle of 28^o, which lies within the funnel flow region.

Designers of silos are most interested in vertical and horizontal pressures on the silo walls, which depending on the behaviour of the silo may change between different regions of the silo and over different time periods. Initially, pressures due to the filling process are known as '*static*' pressures. Active pressure fields develop during filling and the lines of principal stress will be essentially vertical, with the active earth pressure coefficient being less than one and vertical stress magnitudes exceeding the horizontal stress magnitudes and some arching on the walls of the silo. It should be noted that the stress state in the conical hopper section will be slightly different to those in the cylindrical main body of the silo. Pressures that occur during the discharge of the silo are referred to as '*dynamic*' pressures. During discharge principal stress rotations lead to a change to a passive pressure distribution, with horizontal stresses being larger than vertical stresses. '*Switch*' pressures also occur during the transition from static to dynamic stress states, causing transient increases on sections of the silo walls. When the discharge gate at the base of the hopper is opened, material starts flowing and the lines of principal stress in this region become nearly horizontal. The vertical support of the solids near the outlet has been removed, and this material starts to expand vertically downwards, reducing the vertical pressure and causing changes from a static to a dynamic stress field. Arching begins to occur across the zone near the outlet and as more material expands with further discharge, a region of displacement extends upwards and the switch pressures travel up the side of the silo walls (due to a deficiency of wall support during flow). Eventually this displacing column extends up to the free surface of the material in the silo and collapses creating continuous funnel flow, with stagnant zones outside the main displacing discharge.

Theories providing hopper wall pressure estimates were first presented by Walker (1966) followed by Jenike (1961). Jenike (1961 and 1973) proposed the following

equations for the static and dynamic stresses: normal (σ_n), radial (σ_r), angular stresses (σ_Θ) and shear stresses $(\tau_{r\Theta})$. Table 1 gives the stress calculation equations. The dynamic maximum pressure is related to a modified depth-ratio, i_N as shown in Figure 3(c).

$$i_N=\frac{Z_N}{H_h} \quad (1)$$

Where: z_N is the depth of the maximum pressure in the hopper, H_h is the total height of the hopper, k is the stress ratio considered by Jenike, ϕ_w, ϕ_m are the wall and material friction angles, S is the radial stress field, a function of (r and Θ), α is the hopper vertical curvature inclination, Ψ is the angle of inclination of the major principal stress, γ is the unit weight of the material and D_o is the diameter of the orifice.

Table 1: Equations for the Static and Dynamic Pressure

Static Condition
$(\sigma_N)_{static}=\frac{2\gamma H_h \tan(\alpha)}{2*[\tan(\alpha)+\tan(\phi_w)]*(1+\frac{Z_N}{H_h})}$
$\sigma_\Theta=\frac{2k\gamma S i_N H_h}{Cos\Theta(1+k)}$ $\quad$ $\sigma_r=\frac{k\gamma S i_N H_h}{Cos\Theta(1+k)}$
$\tau_{r\Theta}=\sigma_\Theta \tan(\phi_w)$
$k=\frac{\sigma_\Theta}{\sigma_r}<1$ for hopper filling
Dynamic Condition
$(\sigma_N)_{dynamic}=s(\Theta)\gamma D i_N*\frac{\sin(\alpha)}{2}(1-\sin\phi_m \cos 2\Psi)$
$\sigma_\Theta=\sigma(1-\sin\phi_m \cos 2\Psi)$
$\sigma_r=\sigma(1+\sin\phi_m \cos 2\Psi)$
$\tau_{r\Theta}=\sigma \sin\phi_m \sin 2\Psi$
$\tan\phi_w=\frac{(1+k)\sin\alpha}{i_N(1+i_N)2kS}-\tan\alpha$

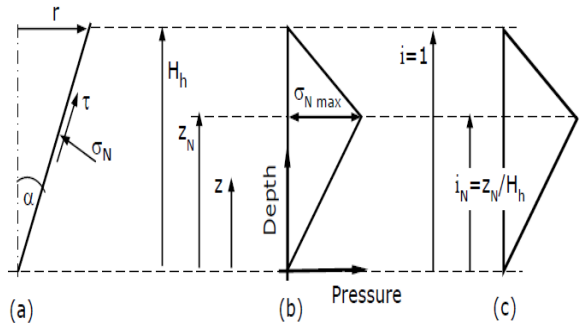

Figure 3: (a) Hopper cross section (b) Normal Pressure (c) Ratio i_N

It should be noted that a silo body may consist of only the vertical wall body and/or an inclined discharge body known as the hopper. Beverloo *et al.* (1961) proposed an equation to estimate the granular mass flow from the outlet of a silo due to 'shear flow':

$$M_f = C\,\rho\sqrt{g}\,(Do-kd)^{5/2} \quad (2)$$

Where: C=Discharge coefficient which depends on bulk density, ρ=soil density, g=gravitational acceleration, D_o=orifice diameter, k=shape coefficient and d=soil particle diameter.

The constant k is, typically $1.3 < k < 2.9$, (Beverloo *et al.*, 1961). The term 'kd' accounts for the wall effect, where the particles do not fully flow at the perimeter of the outlet. C refers to the parameter in relation to free fall or flow of particles through different orifice apertures affecting the mass flow at the orifice level. C is 0.58 for circular openings, or can also be defined as:

$$C=\frac{\sqrt{2\beta\pi}}{4} \quad (3)$$

Where: β=0.5 for a relative proportional arch to aperture ratio $(H_h/D_0 > 1)$ and C=0.58, which is a commonly used value for a circular opening (Bian, 2014).

In this paper, we will attempt to visualize the flow patterns of a model conical hopper under natural gravity using the particle image velocimetry method. Qualitative information on the velocities, strain and shear rates will be extracted from the PIV data. Comparison of the flow patterns across the model will be made to better understand the internal physical mechanisms occurring during material discharge from a classical hopper cross-section.

2 MATERIALS AND METHODS

2.1 Tested Granular Material

Barco B-49 silica sand has been used in this research study as a granular material. This is a sub-angular silica sand. Mechanical tests including grain size distribution, maxmum and minimum void ratios, specific gravity, compaction limits, and direct shear box were carried out on the soil to identify its geo-mechanical properties. Figure 4(a) shows the narrow grain size distribution of the soil. All of the mechanical properties of the tested soil are provided in Table 2. Figures 4(b) and 4(c) give the Direct Shear Test results based on ASTM D3080/D3080M-11 at different normal stresses of 25 kPa, 50 kPa, 75 kPa, 100 kPa and 200 kPa respectively. This shows the peak and critical state failure envelopes for the soil at a relative density of D_r = 20%. The peak dilation angle is seen to reduce with pressure and is relatively constant above pressures of 75

kPa. For the silo tests, the soil was colored using food coloring, and retested to ensure no changes in the aforementioned properties. Even though PIV does not require such provisions to capture particle movement, coloring is used only to visualize the flow patterns for presentation purposes.

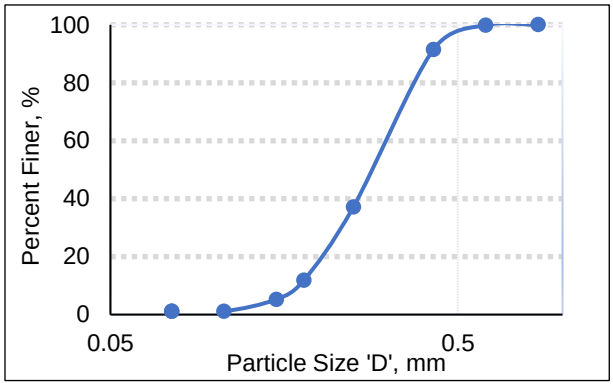

Figure 4(a): Particle size distribution of soil

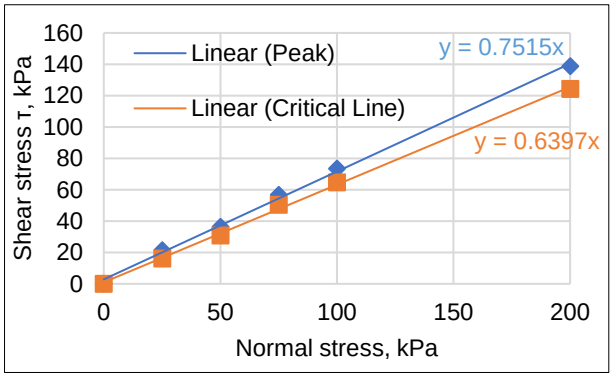

Figure 4(b): Peak and critical state failure envelopes

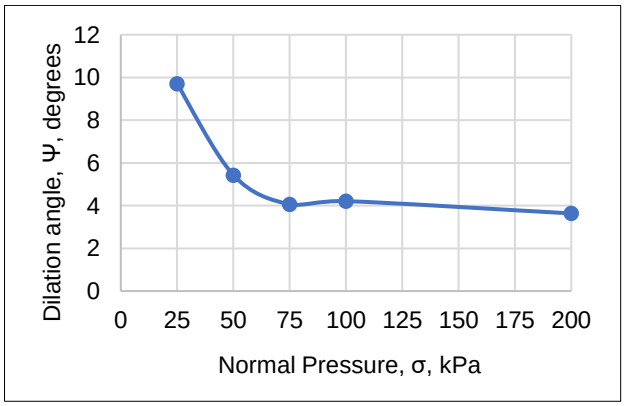

Figure 4(c): Dilation angle variation with normal stress

Table 2: Summary of mechanical properties of tested soil

D_{50}, mm	0.29
Coefficient of uniformity, C_u	1.88
Coefficient of curvature, C_c	0.95
Specific gravity, G_s	2.65
Maximum void ratio (e_{max})	0.68
Minimum void ratio (e_{min})	0.48
Critical state angle of friction, ϕ'_c (º)	32.5

2.2 Hopper Geometry

A half model hopper was considered for the test setup. This was adopted due to the suitability for the PIV image capture of the flow and to prepare for later tests in a centrifuge at different 'g' levels. The cross-section of this model body and the positions of i_N is given in Figure 5. The hopper is closed using a thin plate which is withdrawn to initiate flow.

2.3 Preparation of Silo Hopper and Measurements

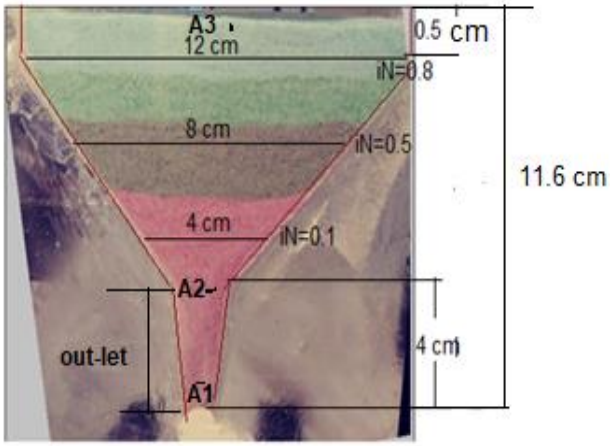

Figure 5: Hopper frontal cross-section and i_N positions

The hopper setup described in this paper was tested at natural gravity (i.e. 1g). It will later be replicated for '10', '25' and '50' g tests to be conducted in a 2.2 m Drum Centrifuge at Western University. Therefore, the hopper is fixed inside a Drum Centrifuge box as shown in Figure-6. The soil is air-pluviated into the hopper to create a uniform unit weight prior to discharge of the model (unit weight, $\gamma = 15.8$ kN/m^3), which corresponds to a relative density $D_r = 20\%$ and a void ratio e=0.64. The hopper is 7.5 cm deep (H_h) down the centreline (A_3-A_2) and has a 1.8 cm orifice size (D_o) at the hopper outlet. Note this cross-section is slightly different to that of a classical hopper due to the additional steep outflow section (A_2-A_1). Most of the information provided during this paper refers to the behaviour in Section A_3-A_2.

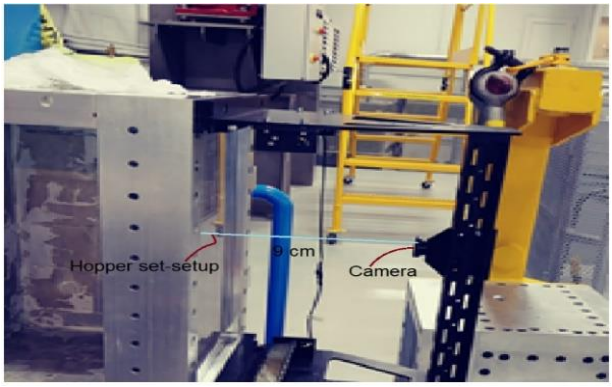

Figure 6: Laboratory test set-up

To perform quantitative analysis of the observed soil behavior, particle velocities must be measured with high accuracy and precision (White *et al.*, 2001). To do this, particle image velocimetry (PIV) analysis was used in this study. PIV analysis is a velocity measuring technique which was originally developed in the field of fluid. This technique can provide the displacement field for an experimental model, as well as strain and stress band measurements over an entire area of interest. PIVlab is an interface in Matlab used to capture deformation properties mostly in liquids using the PIV approach. However, recently, ensemble correlation was added, making PIVLab suitable for micro-PIV which enables an easy approach to capture granular skeleton deformation properties. The results acquired from this analysis partly include shear rate (s^{-1}), strain rate (s^{-1}) and velocity magnitude (mm/s) comprising u and v velocity components. A series of images were taken through the hopper discharge period using a digital camera (EOS 1000D digital camera) placed 9 cm from the experimental setup as shown in Figure 6. The frame rate of the set-up is 94 ms and 10.1 Mega pixels. The camera faces the flat plexiglass surface of the half model hopper for visualizing flow patterns in this region.

3 THEORETICAL RESULTS

3.1 Static and Dynamic Pressures

Figure 7 compares the estimated static and dynamic normal wall pressures. The pressure values in this figure were calculated using the equations provided in Table 1 and the geometry of the hopper presented in Figure 5. This shows the relatively modest changes in active normal stresses that resulted from the filling process at natural gravity. Note the rapid increases in the the wall stresses due to the discharge process (dynamic stress state) which are essentially zero at the discharge orifice and increase up the wall due to arching.

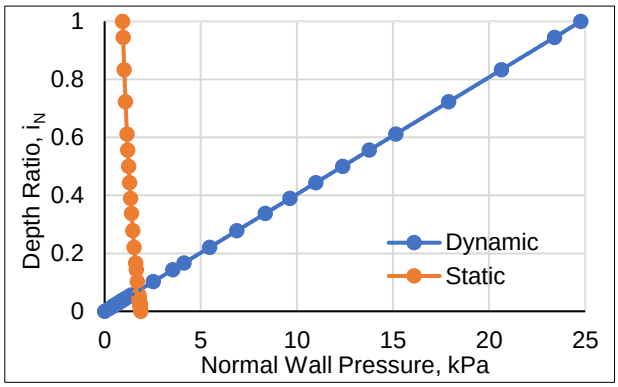

Figure 7: Static and dynamic normal wall pressure

3.3 Granular flow using the Beverloo equation

Based on equation 2, the granular flow, M_f for different orifice diameters is presented in Figure 8. The experimental test results (presented later in the paper) will be compared with the value for a D_o = 1.8 cm exit size with the Beverloo flow calculation in Figure 8, where d is the average diameter of the granular material. Table 3 summarizes the granular material and hopper orifice properties used to estimate the relationship between mass flow and orifice diameter as shown in Figure 8.

Table 3: Granular flow calculation parameters

C	ρ (kg/m^3)	g (m/s^2)	k	d (mm)	D_r	ϕ'_c
0.58	1.58	9.81	2.5	0.28	20%	32.5^o

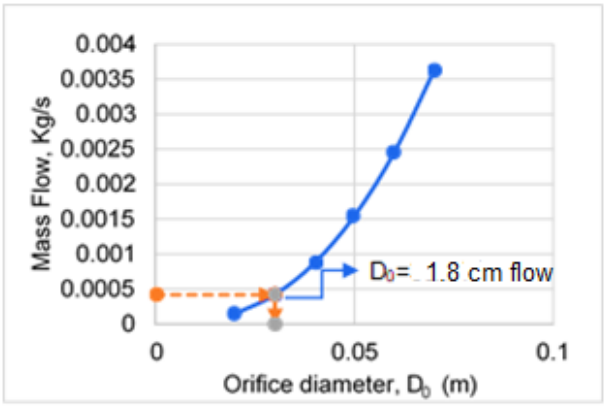

Figure 8: Theoretical silo granular flow rate

This analysis suggests that the experimental hopper will have a constant outflow rate of 0.0005 kg/s.

4 EXPERIMENTAL RESULTS

4.1 Qualitative behaviour from video images

Figure 9 shows the different stages of the discharge for the hopper (a to f). In each case, the disturbance of the initially horizontal coloured sand layers shows qualitatively the zones of material disturbance. These images represent the following time periods (in seconds) after the discharge commenced t_1 to t_6 = 94 ms to 376 ms.

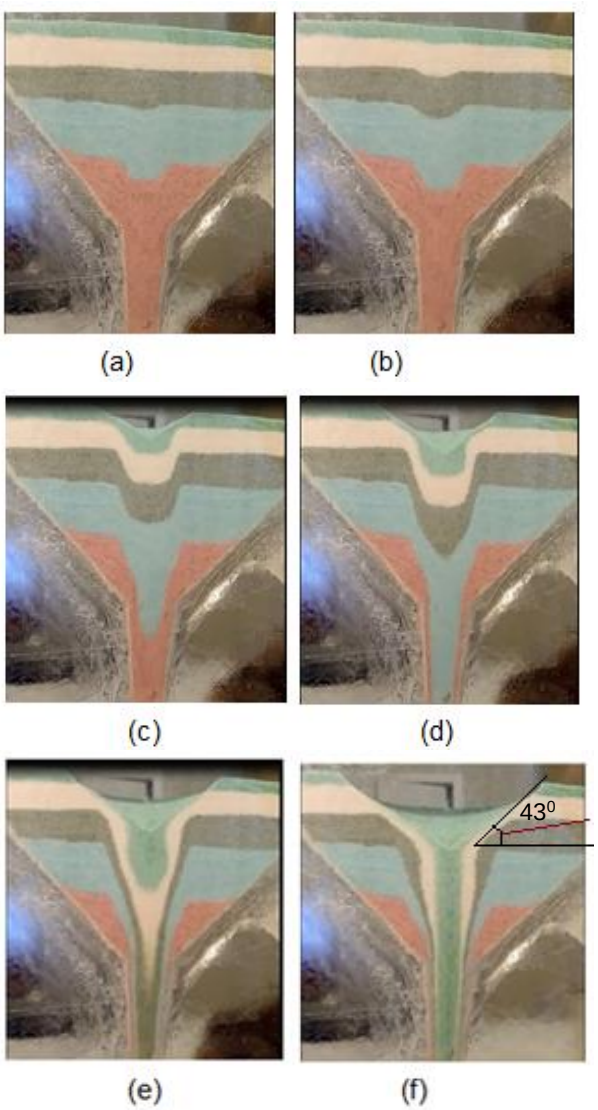

Figure 9: Images showing development of funnel flow

The first two images (a and b) show the flow immediately after discharge from the outlet starts. The images show a downwards moving central core (or funnel) flow, whose extent is propagating vertically upwards with time and what appears to be distinct velocity discontinuities at the edges. The curved displacement regions in the central core suggest the highest velocity is occurring down the centreline of the hopper. In both images a and b, the upper free surface does not appear to have been influenced by this process.

Images c and d show the central flowing core reaching the upper free surface and the initiation of a surface depression, which broadens with time. The collapse of the central core/column of the soil is more evident in these images as the material exits the hopper. Stagnant zones of soil exist on either side of the flowing core with relatively steep face angles, showing the effects of arching against the walls of the hopper. The stagnant zones are seen to terminate at the orifice edges and the soil has low velocities in these regions. The final two images e and f show the transition to fully developed funnel flow. The depression of the upper surface continues to increase in depth and breadth, with a slope angle approximately that of the critical state friction angle of the soil. It should be noted that the material from the uppermost layers is exiting the outlet, whilst a significant portion of the material near the sides of the hopper is still in place, with no relative downward movement. The following sections will utilise PIV to further understand the flow fields and the material behaviour during hopper discharge.

4.2 Particle Image Velocimetry

Figure 10a shows the velocity vectors corresponding to Figure 9b and shows column of flowing soil that is propagating vertically upwards through the hopper just after discharge commences. This shows a very localised flow mechanism with near vertical sides and stagnant material adjacent has likely transitioned to a passive stress state. The curved upper portion of the displacing column is an interesting feature and suggests further soil arching above the column. The velocity vectors are generally aligned with the vertical direction, but it is evident that the flow field is not completely uniform and suggests much turbulence is occurring in the flow during discharge. This appears to be predominantly concentrated in the region near the outlet.

In Figure 10b corresponding to Figure 9(f), the column is seen to reach the upper soil surface and then collapse with an almost constant velocity funnel (central core flow). As this occurs the upper zone develops into an inflow zone, with predominantly radial vectors that rotate to vertical directly above the flowing funnel. The upper surface appears to be nearly conical during the final stages of emptying. Previous work with discrete element analysis (Mollon and Zhao, 2013) suggest that rough angular particles have narrower more intense funnel flow regions. For both spherical and angular particles, near the outlet there is a region of high rotational velocity due to the change in flow regime in proximity with the outlet. Above this region of high disturbance, rotations are less intense. The coordination number (i.e. number of contacts per grain) is found to decrease in this lower zone and thus the grain rotations are due to loss of contacts and rotational interlocks between grains. The stress fields found in the discrete element analysis suggest high stresses occur at the walls and this implies the action of arching, which is enhanced in angular particle distributions that allow force chains to develop more strongly and deviate from the purely normal direction. On a macroscopic scale, this

corresponds to an increase of the friction angle. Despite the high dilatancy of the soil found at very low stresses in the direct shear tests, the inclinations of the discontinuities between the stagnant zones and the central flowing core are much higher than would be expected based on the single element laboratory testing.

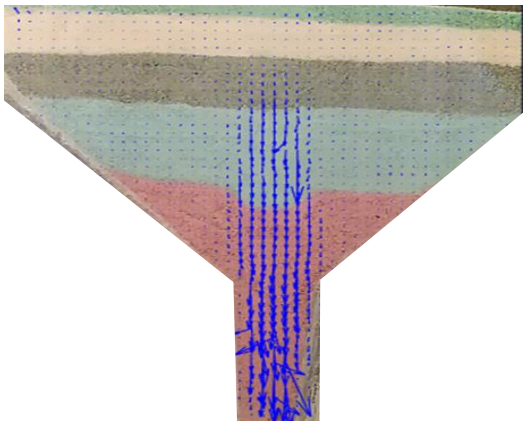

(a)

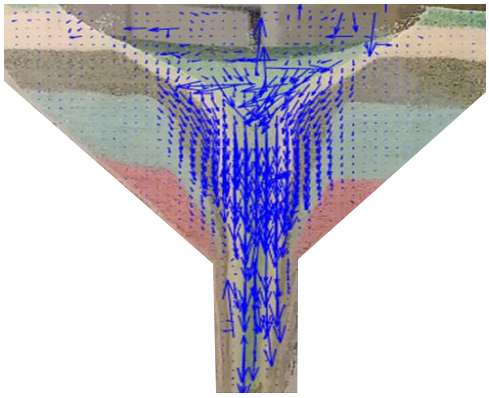

(b)

Figure 10: (a) and (b) PIV derived soil flow mechanisms

4.3 Velocity profiles across the model

Two profiles for the vertical velocity across the horizontal and vertical planes of the model during the later stages of outflow are shown in Figure 11. Due to the rapidly changing velocity profiles, these figures are an average of three 94 ms images. The horizontal plane (taken at the level corresponding to i_N=0.8) is shown in Figure 11a and shows a symmetrical velocity profile across the model with the peak velocities occurring in the centre of the funnel. These velocities reduce significantly with distance from the symmetry axis. This type of behaviour has been successfully modelled previously with a Gaussian distribution of velocities (Choi et al., 2005).

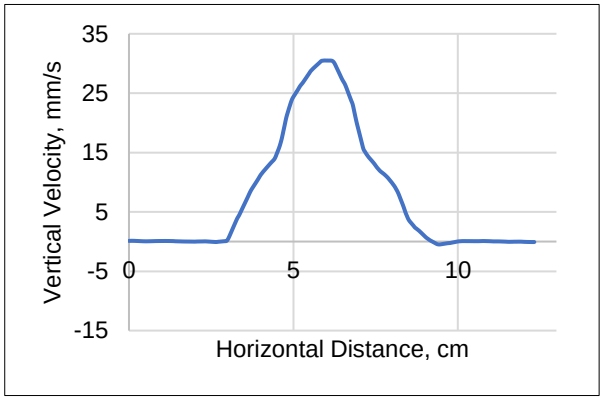

Figure 11(a): Vertical velocity profiles

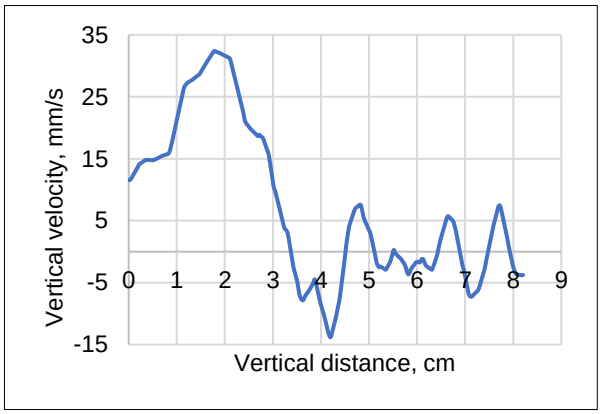

Figure 11(b): Vertical velocity profiles

The vertical profile shown in Figure 11b, shows the peak vertical velocities down the centreline of the model occur just below the conical shaped surface depression, which decrease significantly towards the base of the conical section of the model. This contrasts with typical hopper observations, where the highest velocities are seen near the outlet. This is believed to be due to the presence of the lower outflow section, which may be impeding the outflow somewhat. Further testing will be conducted with this section removed, to confirm this hypothesis. It should also be noted that there is significant disturbance of the flow field near the outlet, suggesting more time steps should be averaged to guarantee more accurate estimates of outflow velocity. Based on a number of observations of the outflow from this region, the mass flow from the model is 0.00048 kg/s, which compares to 0.0005 kg/s from Section 3.3 of the paper using the Beverloo equation results in Figure 8.

4 SUMMARY AND CONCLUSIONS

Particle Image Velocimetry (PIV) based experimental tests have been used to investigate the granular flow properties in a half model smooth-sided silo hopper. The study of granular silo flow dynamics due to gravity has been commonly done to understand pressure effects on the walls of the hopper and flow rate at the exit of the hopper.

This paper has shown that the flow patterns and dynamic flow properties of a model silo system under natural gravity can be effectively captured using PIV. Although numerical modeling simulations exist for silo and hopper granular flow analysis, PIV appears to be a valuable additional tool for practical and experimental capture of the actual material flow. Hoppers operate in the intermediate regime between quasi-static yield and rapid frictional flow, and the flow behaviour is also influenced by non-continuum effects, such as local packings (Potapov and Campbell, 1996). Hence it is extremely difficult to analytical or numerically model the behaviour. Therefore, the development of experimental methods is particularly important.

The results in the paper show that the flow mechanisms in a silo are quite complex and vary temporally and spatially. The results are qualitatively similar to those of other researchers for model systems. Three distinct zones of behaviour were observed: a) an upper inflow zone, b) a narrow vertical funnel flow zone and c) a near static stagnant zone. The characteristics of these flow zones are likely to be influenced by the material and geometric properties of the silo. Additional testing will be conducted by the researchers with other materials, silo geometries and enhanced gravities in the centrifuge, to further understand the physical processes involved and the limitations of the experimental methods. There is also some scope to combine the PIV velocity data with standard mechanical relationships to better quantify the stress fields during discharge of the silo.

5 REFERENCES

Barbir, O. and Mathews, J. (2016). Investigation of the influence of gravity on granular flow using silo centrifuge model. *EYGEC 2016*, Sibiu, Romania, 3-4.

Beverloo, W.A., Leniger, H.A., and Van der Velde, J. (1961). The Flow of Granular Solids Through Orifices. *Chem. Engrg. Sci.*, 15: 260-264.

Bian, Q. (2014). *Bulk flow properties of wheat*. Department of Grain Science and Industry College of Agriculture Kansas State University Manhattan, Kansas.

Bransby, P.L. and Blair-Fish, P.M. (1974). Wall stress in mass flow bunkers. *Chem. Eng. Sci.* 29: 1061-1074.

Brennen, C.E. (2005). *Fundamentals of multiphase flow*. California Inst. Technology, Cambridge University Press.

Caram, H. and Hong, D.C. (1991). Random walk-approach to granular flows. Phys. Rev. Lett. 67(828): 5-9.

Choi, J., Kudrolli, A. and Bazant, M.Z. (2005). *The spot model for random packing dynamics*. Department of Mathematics, Mass. Institute of Technology, 12-13.

Davidson, J. F. and Harrison, D. (1974). Fluidization. *Science Progress.* 61(242): 191-217.

Hughes, F.E. and Madabhushi, S.P.G. (2019). Liquefaction Induced Displacement and Rotation of Structures with Wide Basements. *Soil Dyn & Earthqke Eng*. 120: 75–84.

Hutter, K.M. Savage, S.B. and Nohguchi, Y. (1993). Two-dimensional spreading of a granular avalanche down an inclined plane Part I, 37-44.

Iverson, R.M. (1997). *The physics of debris flows.* Cascades Observatory U.S. Geol. Sur., Washington.

Jenike, A.W. (1961). *Gravity Flow of Bulk Solids.* Bulletin 108, Utah Engineering Experiment Station, University of Utah, Salt Lake City, October.

Jenike, A.W. (1968). Bins Loads. *Journal of the Structural Division, Proc. Am. Soc. of Civil Engineering*, 1014-1040.

Litwiniszyn, J. (1963). The model of a random walk of particles adapted to researches on problems of mechanics of loose media. *Bull. Acad. Pol. Sc. Ser. Tech.* 11: 61–70.

Mathews, J.C. and Wu, W. (2016). Model tests of silo discharge in a geotechnical centrifuge. *Powder Technology*. 293: 3-14.

Medina, A., Córdova, J.A., Luna, E. and Treviño, C. (1998). Velocity field measurements in granular gravity. *Physics Letters A*. 250: 111-116.

Mollon, G. and Zhao, J. (2013). Characterization of fluctuations in granular hopper flow. *Granular Matter.* 15 (6): 3-7.

Mullins, W.W. (1972). Stochastic Theory of Particle Flow under Gravity. *Journal of Applied Physics*. 43: 665-669

Nedderman, R.M. and Tüzün, U. (1979). A Kinematic Model for the Flow of Granular Materials. *Powder Technology*. 6-10.

Nielsen, J. and Askegaard, V. (1977). Scale errors in model tests on granular media with special reference to silo models. *Powder Technology*. 16(1): 123—130.

Nortje, D. (2002). *The Anti-Dynamic Tube in Mass Flow Silos*. PhD Thesis to the University of Western.

Ooi, J.Y., Chen, J.F. and Rotter, J.M. 1998. Measurement of solids flow patterns in a gypsum silo. *Powder Technology*. 99(3): 272-284.

Pitman, E.B. and Schaeffer, D.G. (1987). Two phase flows and waves, *Commun. Pure Appl. Math*. 40: 421-447

Potapov, A.V. and Campbell, C.S. (1996). *Computer simulation of hopper flow*. Dept of Mech Eng, Uni of Southern California, 90089-1453: 9-11.

Prakash, J. and Rao, K. (1991). Velocity profile of granular flows inside silos and hoppers. *J. Fluid Mech.* 8-13.

Rotter, J.M., Jumikis, P.T., Fleming, S.P., and Porter, S.J. (1989). Experiments on the buckling of thin-walled model silo structures. *Journal of Constructional Steel Research.* 13(4): 271-299.

Schulze, D. (2007). *Powders and Bulk Solids – Behavior, Characterization, Storage and Flow.* Springer Berlin.

Shook, C.A. and Roco, M.C. (1991). *Slurry Flow: Principles and Practice*. Butterworth-Heinemann.

Walker, D.M. (1966). An approximate theory and theory for pressures and arching in hoppers. *Chemical Engineering Science*. 21: 980-991.

White, D. and Take, A.W. (2002). *GeoPIV: Particle Image Velocimetry (PIV) software for use in geotechnical testing.* London: Cambridge University Eng Department.

Yong, H.W. (1990). *Static and Dynamic Analysis of Flow of Bulk Materials through Silos*. University of Wollongong Thesis Collection, 6-10.